Secondary Structure and Temperature Behavior of the Acetylcholine Receptor by Fourier Transform Infrared Spectroscopy†

Dieter Naumann,*,‡ Christian Schultz,‡ Ute Görne-Tschelnokow,§ and Ferdinand Hucho§

Robert Koch-Institut des Bundesgesundheitsamtes, Nordufer 20, D-1000 Berlin 65, FRG, and Institut für Biochemie der Freien Universität, Berlin, Thielallee 63, D-1000 Berlin 33, FRG

Received March 24, 1992; Revised Manuscript Received December 15, 1992

ABSTRACT: Fourier transform infrared spectroscopy (FT-IR) was used to test the secondary structure of purified acetylcholine receptor membranes from *Torpedo californica*. The secondary structure was estimated using the spectral features observed in the structure sensitive region of amide I and amide I′ (between 1600 and 1700 cm^{-1}), taking advantage of Fourier self-deconvolution and second-derivative techniques along with least-squares band fitting procedures. At least six different amide I′ band components could be resolved in D_2O and were tentatively assigned to β-structures (1680 and 1636 cm^{-1}), α-helices (1657 cm^{-1}), aperiodic structures and/or distorted helices (1646–1648 cm^{-1}), and turns (1690 and 1668 cm^{-1}), respectively. The β-band around 1637 cm^{-1}, in particular, turned out to be complex since it reproducibly exhibited weak features near 1630 and 1627 cm^{-1}, thereby suggesting the presence of different chain interacting β-structures. The band near 1657 cm^{-1} was assigned to α-helices which traverse the membrane bilayers, while 1646–1648-cm^{-1} component was tentatively attributed to aperiodic structures and α-helices localized within the "globular head" of the receptor protein protruding from the membrane surface into the surrounding water. Least-squares band fitting procedures were applied in order to estimate relative amounts of secondary structures. The results suggest 36–43%, 32–33%, 14–24%, and 18–19% for β-, α-helical, turn, and "rest" structures, respectively. Additionally, the temperature- and time-dependent variations of the secondary structure was tested by evaluating the changes of amide I and amide II band components of receptor membranes dispersed in H_2O and D_2O. The results are indicative of differing stability of the various protein secondary structures. The known activity loss of AChR membranes at temperatures above 20 °C correlates well with considerable isothermic changes of β-, aperiodic, and small loss of α-helical structures.

Reports on the secondary structure of the AChR complex available from the literature are rare. The reported results differ significantly: Circular dichroism spectroscopy (CD)[1] suggested 34% α-helices, 26–32% β-sheets, and 34–40% "aperiodic" conformations (Moore et al., 1974), 24% α-helices, 41% β-structures, and 28% random conformations (Mielke & Wallace, 1988), or 35–44% helices, 18–37% β-structures, 0–10% turns, and 19–32% random structures (Wu et al., 1990). Raman-spectroscopic analysis yielded 34% antiparallel β-sheets, 25% ordered α-helices, and 16% distorted helices, 15% turns and 10% "undefined" conformations (Aslanian et al., 1983; Yager et al., 1984). Recent FT-IR investigations using affinity-purified, reconstituted AChR/lipid systems suggested 25% α-helical and 28% β-structure using two conformation-sensitive IR bands in the so-called skeletal region of the IR spectrum (Fong & McNamee, 1987). These values are rather ambigious because of the artificial system used (AChR reconstituted at a lipid/protein ratio of 200–400, as opposed to about 0.5 in the native membrane). The latter authors also reported on the ratios of α-helical and β-structures as a function of temperature and composition of the lipid bilayer matrix. Both parameters were suggested to be raised to the channel activity of the AChR complex.

Because of the lack of appropriate crystals, the three-dimensional structure of the AChR as determined by X-ray crystallography is not yet known. Secondary structure prediction, initially performed for the γ-subunit (Claudio et al., 1983), based on hydrophobicity analysis according to Kyte and Doolittle (1982) and Fourier analysis of the hydrophobicities of the four different receptor subunit sequences (Finer-Moore & Stroud, 1984; Stroud et al., 1990), led to several proposals as to the transmembrane folding of the polypeptide chains. These models, refined on the basis of immunochemical [reviewed in Claudio (1989)] and chemical (DiPaola et al., 1989) studies, now agree that each of the five subunits traverses the membrane bilayer by means of four α-helical segments, both the N- and C-terminus being located on the extracellular side of the membrane. These transmembrane helices most probably play a functional role in the signal transduction from the agonist binding site, located on the extracellular side of the receptor, to the gating structure of the ion channel, most likely located close to the intracellular face of the membrane (Hilgenfeld & Hucho, 1989). Although these structure models are widely accepted, one has to keep in mind that they represent only predictions. In the absence of high-resolution X-ray data, spectroscopy is able to provide structurally relevant data.

We report here on some results of a recent FT-IR analysis of the conformation-sensitive amide I and amide II band contours of purified, AChR-rich membranes of *Torpedo californica*. In order to obtain reliable information on the number and positions of underlying component peaks relevant for qualitative and quantitative assessment of secondary structure, second-derivative, Fourier-self-deconvolution, difference spectroscopic and band-fitting procedures were applied. Some tentative assignments of the various amide I component

† This work was supported by grants from the Deutsche Forschungsgemeinschaft (SFB 312) and the Fonds der Chemischen Industrie.

* Author to whom correspondence should be addressed.

‡ Robert Koch-Institut des Bundesgesundheitsamtes.

§ Institut für Biochemie der Freien Universität.

[1] Abbreviations: AChR, acetylcholine receptor; CD, circular dichroism; DMPA, 1,2-dimyristoyl-*sn*-glycero-3-phosphatic acid; DMPC, 1,2-dimyristoyl-*sn*-glycero-3-phosphocholine; DMPE, 1,2-dimyristoyl-*sn*-glycero-3-phosphoethanolamine; FT-IR, Fourier transform infrared; IR, infrared.

0006-2960/93/0432-3162$04.00/0

bands to specific secondary structure elements are proposed, which may help to interpret the difference spectroscopic peaks recently observed by FT-IR between the resting and the desensitized state of AChR (Görne-Tschelnokow et al., 1992; Baenziger et al., 1992). Additionally, the temperature stability of AChR is tested by collecting FT-IR difference spectra along a linear temperature gradient and, time-dependently, at constant temperatures.

MATERIALS AND METHODS

Purified, AChR-rich membranes from *T. californica* were prepared according to the protocol described by Schiebler and Hucho (1978). The membranes obtained after sucrose density gradient centrifugation were washed twice with cold water or D_2O to remove sucrose and, for D_2O, to replace exchangeable hydrogens with deuterium. The D_2O/membrane dispersions were kept for 24 h at 4 °C and were again centrifuged; the supernatant was then discarded and fresh D_2O added. The H_2O and D_2O dispersions were pelleted with an airfuge (Beckmann) to yield a membrane concentration of approximately 5% (w/v). The pellets were than transferred to a temperature-controlled, home-made IR-cuvette system equipped with CaF_2 windows and 8- and 50-μm Sn spacers for the H_2O and D_2O samples, respectively. The temperature-dependent FT-IR spectra were collected on a 10-MXE FT-IR spectrometer from Nicolet Instruments, (Madison, WI) (equipped with a TGS detector). The spectra for resolution enhancement experiments were obtained on an IFS-66 FT-IR spectrometer from Bruker Instruments (Karlsruhe, FRG) (equipped with a DTGS detector). In both cases resolution was set to 4 cm^{-1}, and data point resolution was approximately 1 data point per wavenumber. A Happ-Genzel apodization function was applied for Fourier transformation of interferograms, and approximately 108 (Nicolet 10MX-E) and 512 (Bruker IFS 66) interferograms were collected and averaged for spectral data acquisition. Spectral derivatives were calculated using a Savitzky-Golay algorithm applying a nine-point approximation. Fourier self-deconvolution was performed using a similar algorithm as described by Kauppinen et al. (1981). For band fitting the amide I contour, the following procedures were used: (i) The spectra were corrected for spectral contributions of H_2O or D_2O between 1800 and 1500 cm^{-1}. (ii) The spectra were deconvolved using an initial Lorentzian line-shape function with full bandwidth at half-height of 20 cm^{-1} and a resolution enhancement factor of 2.5. (iii) Band curve fitting was performed between 1700 and 1500 cm^{-1} using a nonlinear least-squares fitting procedure based on the Marquardt algorithm (Marquardt, 1963). The program GAUSSFIT written in Turbo-Pascal was installed on a 32-bit PC Dell 325D. For temperature-dependent measurements, a linear temperature gradient of 1 °C temperature increase per 5 min was applied while continuously recording and storing the FT-IR spectra. Evaluation of frequency shifts was done as described (Naumann et al., 1989).

RESULTS AND DISCUSSION

Figure 1 depicts the typical survey FT-IR spectra of AChR membranes dispersed in H_2O and D_2O after solvent substraction, respectively. In case of the D_2O dispersions, residual amide II band intensity was retained near 1548 cm^{-1} which was due to the slowly exchanging or nonexchanging amide N–H hydrogens in highly ordered structures and/or in domains of the protein that are sheltered from rapid solvent exchange. FT-IR is particularly sensitive to different hydrogen-bonding patterns, to different H/D exchange rates of these structures,

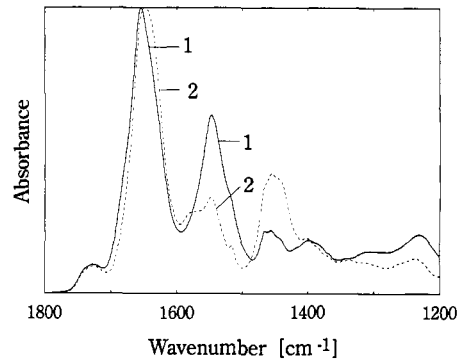

FIGURE 1: Typical survey FT-IR spectra of AChR membranes after solvent substraction. (1) AChR membranes dispersed in H_2O. (2) AChR membranes dispersed in D_2O.

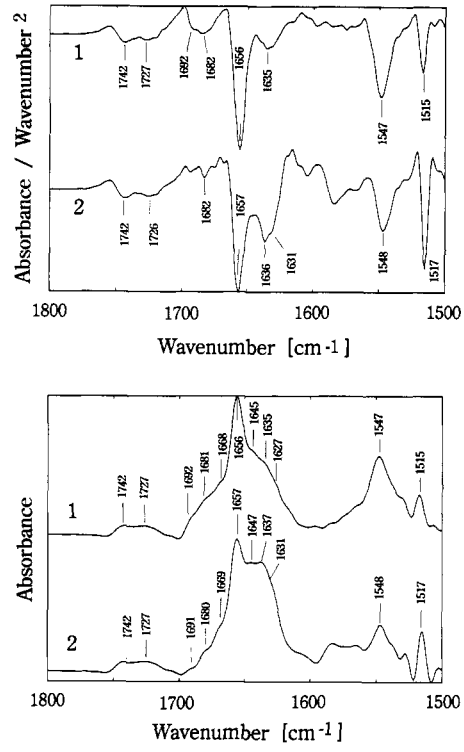

FIGURE 2: Resolution-enhanced amide I and amide I′ band contours of receptor-rich membranes as obtained by different band-narrowing procedures. (top) Second-derivative spectra as calculated by a nine-point Savitzky/Golay algorithm (spectrum 1 from AChR in H_2O; spectrum 2 from AChR in D_2O). (bottom) Fourier self-deconvolved spectra using a Lorentzian line-shape function with a 20-cm^{-1} full width at half-height and an enhancement factor of 2.5 (spectrum 1 from AChR in H_2O; spectrum 2 from AChR in D_2O). These have been corrected for the D_2O background but not for possible small contributions from amino acid side-chain contributions and from the membrane matrix itself. The major natural constituents of the AChR membrane are assumed to be DMPC, DMPE, DMPA, and cholesterol. These compounds do not exhibit specific IR features between 1610 and 1700 cm^{-1}.

and to different accessibilities of solvent to the shielded or interior parts of a protein. The intensities of absorbance of amide II and amide I bands, in particular, can be used to estimate the fraction of unexchanged amide protons according to the relationships described elsewhere (Downer et al., 1986). From similar evaluations, a fractional amount of nonexchangeable hydrogens of 30–35% was estimated on the basis of the spectra shown in Figure 1. Figure 2 depicts the spectra of Figure 1 in the 1500–1800-cm^{-1} region after digitally calculating the derivative and Fourier-deconvolved spectra. Both resolution enhancement techniques revealed a series of

Table I: Assignment of Some IR Absorption Bands Observed in the 2800–3100 and 1500–1800 Wavenumber (cm^{-1}) Regions of the FT-IR Spectra of AChR-Rich Membranes

frequency (cm^{-1})	tentative assignment
3010	C=C–H stretching
2956	asymmetric $-CH_3$ stretching
2928	asymmetric $>CH_2$ stretching
2875	symmetric $-CH_3$ stretching
2850	symmetric $>CH_2$ stretching
1742	>C=O stretching
1727	ester functional groups
1610–1700	amide I components (>C=O stretching)
1520–1610	amide II (N–H in-plane bending; amino acid side chain vibrations; asymmetric stretching of carboxylate)
1515	"tyrosine"

distinct absorption bands. Some important bands observed between 2800 and 3100 and 1500 and 1800 wavenumbers (cm^{-1}) are tentatively assigned in Table I.

The infrared spectra of AChR membranes displayed significant changes of amide I band contour and a dramatic reduction in the intensity of the amide II band near 1548 cm^{-1} when passing from H_2O to D_2O. The frequency of the major amide I band component near 1656 cm^{-1}, however, turned out to be constant. While significant intensity loss was found for the high-frequency components between 1690 and 1670 cm^{-1}, considerable intensity increase was observed near 1646–1648 cm^{-1} when the sample was passed from H_2O to D_2O solution. The number and individual frequencies of most component bands of amide I, however, were found to be very similar for H_2O and D_2O dispersions. This seems to be typical for membrane proteins which are not completely H/D-exchanged (He et al., 1991).

Assignment of Some Conformation-Sensitive IR Bands of the Acetylcholine Receptor Membranes. The FT-IR spectra of fully hydrated AChR membranes provided several characteristic IR absorption bands which can be used to monitor conformational changes of the AChR complex and its bilayer matrix. The spectral region from 2800 to 3100 cm^{-1} is clearly dominated by the various characteristic C–H stretching bands of the fatty acids of the membrane matrix and by some aromatic C–H stretching bands of phenylalanine, tryptophan, and tyrosine (spectra not shown, see Table I).

The spectral region between 1500 and 1700 cm^{-1} provides the secondary structure sensitive features of the amide I and amide II band and some characteristic amino acid side-chain vibrations. Amide I is essentially due to >C=O stretching vibration, weakly coupled with C–N double-bond stretching and in-plane bending of the planar amide group. The amide II band arises from in-plane N–H bending strongly coupled to C–N stretching vibrations. Both amide bands, especially however amide I, are related to specific secondary structures of the peptide chains (Krimm, 1962; Chirgadze & Nevskaya, 1976; Nevskaya & Chirgadze, 1976; Bandekar & Krimm, 1979, 1980).

The various amide I band components detectable by derivative and Fourier self-deconvolution techniques revealed a complex assembly of different secondary structures. A certain variability between independent preparations of the AChR-enriched membranes was observed. The following secondary structure classes, however, were always detected:

An α-helical band constantly localized near 1656 cm^{-1} in H_2O and D_2O solution. In D_2O this band seemed to be composed of a single, pure helical component. The very perculiar band near 1646–1648 cm^{-1} observed in D_2O was tentatively assigned to be at least in part due to a different type of α-helical structure, though the frequency of this band falls within a frequency range where IR band components are usually assigned to "unordered" or "undefined" structures. We base this interpretation on the following assumptions: (i) The component near 1647 cm^{-1} seems to be rather sharp; "unordered" structures should exhibit much broader bandwidths and are suppressed by the band-narrowing procedures used here; (ii) the component band is localized at frequency values too high to be exclusively due to random structures; (iii) similar low-frequency helical components were detected for Ca^{2+}-ATPase of sarcoplasmic reticulum (1650 cm^{-1}) (Arrondo et al., 1987), for K^+, Na^+-ATPase of *T. californica* (1649 cm^{-1}) Naumann et al., unpublished results), for myoglobin (1649 cm^{-1}) Naumann et al., unpublished results), and for the acetylcholine esterase of *T. californa* (1648 cm^{-1}) (Görne-Tschelnokow et al., unpublished results). We propose that the 1657-cm^{-1} band is related to the helices traversing the bilayer matrix, whereas the 1646–1648 cm^{-1} band is ascribed to "aperiodic" structures and to, e.g., charge-interacting α-helices (Nevskaya & Chirgadze, 1976), presumably localized within the "globular head" of the receptor protein protruding from the membrane surface into the surrounding water. Recent FT-IR measurements suggest that bands at 1645–1648 cm^{-1} may be due to "β-bend ribbon" conformations as well (Kennedy et al., 1991).

The main β-band observed at 1637 cm^{-1} in D_2O exhibited weakly expressed features near 1631 and 1627 cm^{-1}, thus indicating the presence of different interchain hydrogen-bonded β-structures: 1637 cm^{-1} weakly, 1631 cm^{-1} medium, 1627 cm^{-1} strongly interacting β-chains [a pronounced sharp band near 1680 cm^{-1}, together with a prominent band around 1630 cm^{-1}, is usually taken as diagnostic for the presence of β-structures of the antiparallel type of pleated sheet structure (Chirgadze & Nevskaya, 1976)]. Turn- or bend-like structures are supposed to be observed near 1660–1670 cm^{-1} and, to some extent, near 1680 and 1690 cm^{-1}, respectively (Bandekar & Krimm, 1979, 1980; Byler & Susi, 1986).

Quantitative Estimation of the Secondary Structure of Acetylcholine Receptor Membranes. Curve fitting of the deconvolved amide I band contour by partial least-squares fitting techniques is commonly used to estimate the secondary structure of a given protein (Byler & Susi, 1986; Surewicz & Mantsch, 1988).

This technique implies the described three steps of analysis: (i) separation of the overlapping amide I component bands by resolution enhancement, (ii) assessment of the number and positions of underlying component peaks and assignment to known conformational structures, and (iii) quantitation of secondary structure by band profile curve fitting.

While the problems and caveats associated with this technique have been described (Mantsch et al., 1989; Surewicz & Mantsch, 1988), we feel that this approximation is useful in the case of secondary structure analysis of native AChR, since it may provide the quantitative estimation of protein secondary structure and the assignment of specific secondary structure elements to its amide I component bands (Prestrelski et al., 1991) and since it can even discriminate between different α-helices and different hydrogen-bonded β-structures. Thus, our results may also help to clarify the FT-IR difference spectroscopic peaks obtained by the recently published new technique of analyzing the resting to desensitized state transition of AChR (Görne-Teschelnokow et al., 1992).

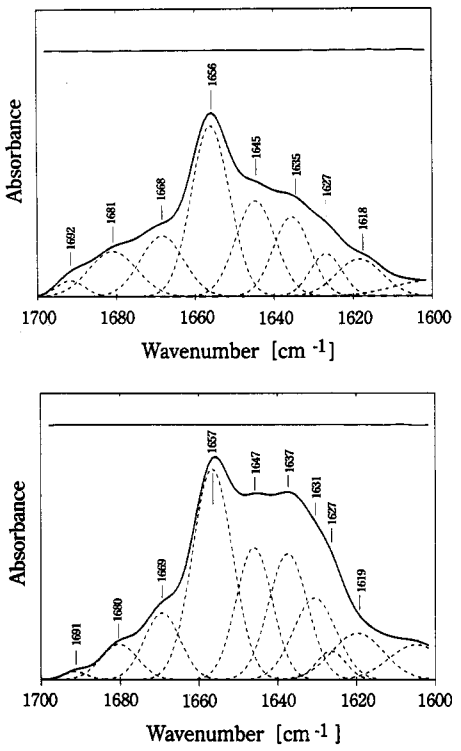

FIGURE 3: Deconvolved amide I and amide I' band contours and the best-fitting individual component bands. (top) AChR membranes dispersed in H_2O. (bottom) AChR membranes dispersed in D_2O. The line at the top of each figure represents the scaled difference spectrum of the original minus the fitted contour.

Table II: Fractional Areas of the Component Bands and the Percentages of Secondary Structures As Found for Purified AChR-Rich Membranes in H_2O and D_2O

H_2O			D_2O		
band component (cm^{-1})	percent	assignment[a]	band component (cm^{-1})	percent	assignment[a]
1692	2.0	B	1691	1.0	B
1681	11.0	T/B	1680	5.0	B/T
1668	13.0	T	1669	9.0	T
1656	33.0	A/R	1657	32.0	A
			1647	18.0	R/A*
1645	19.0	B*	1637	18.0	B
1635	15.0	B	1631	14.0	B
1627	7.0	B	1627	3.0	B

[a] Abbreviations: β, β-pleated sheet structures; B*, β-extended structures (only weakly interacting via interchain hydrogene bonding); T, turn structures; A, α-helical structures (membrane spanning); A*, α-helices (in the globular domain); R, random or "aperiodic" structures.

The variability obtained in the curve fitting with the independent AChR preparations was on the order of ±2–4%, depending on the individual amide I component band. Typical examples of curve fitting results of the receptor complex in H_2O and D_2O are given in Figure 3, top and bottom panels, respectively. The quantitative results of curve fitting are summarized in Table II. In general, the relative fractions of α-helical and β-pleated sheet structures were found to be similar in both H_2O and D_2O dispersions. If one accepts that the band near 1657 cm^{-1} is due to the α-helices which traverse the membrane bilayer and which are not deuterated in the D_2O samples (an amide II "rest band" found near 1548 cm^{-1} and the frequency stability of the 1657-cm^{-1} band provide strong evidence for this assumption), then the total amount of β-structures, α-helices (membrane spanning), turns, and helices localized in the globular domain and/or "rest structures" can be quantified as 36–43%, 32–33%, 14–24%, and 18–19%, respectively. These numbers suggest that β-structures dominate the secondary structure of the receptor complex. While the amount of about 32–33% α-helices obtained from band fitting of amide I is in good accordance with the fraction of unexchangable amide II protons as determined by FT-IR in this work, with CD results published by Moore et al. (1974) and with Raman data published by Yager et al. (1984), recent CD measurements suggested significantly higher and lower fractions of α-helices and β-structures, respectively (Wu et al., 1990). Higher relative amounts of α-helical conformations can only be achieved by the FT-IR technique used in this study, if one accepts that the 1646–1648-cm^{-1} component band observed in D_2O is, at least partially, due to a specific type of helical conformation.

It is known that most authors who published relevant data on the secondary structure of the AChR used samples which have been purified by affinity chromatography and have been modified by reconstitution [see, e.g., Fong and McNamee (1987) and Wu et al. (1990)]. The problems arising from the artificial conditions involved in the various techniques for isolation, purification, and reconstitution of AChR are known [see, e.g., Krikorian and Bloch (1992)] and may, at least in part, account for the different results obtained by the various groups. Apart from this fact, the different analytical techniques used by the authors may also yield differing results. While, e.g., the routinely used CD techniques for estimating the secondary structure of proteins in solution may yield reasonably accurate numbers on α-helical content, it is less accurate for quantitative determination of other secondary structure elements such as β-structures and cannot distinguish between different types of α-helices or between different types of β-structures. Moreover, membrane proteins are difficult to study due to light scattering of the membrane fragments and vesicles. Concerning FT-IR as a means for secondary structure analysis, we would not prefer the method used by Dong et al. (1990), since it is solely based on the methodologically doubtful use of second-derivative signals for quantitation of secondary structures. Recently, alternatives to resolution enhancement of amide I and curve fitting have been developed by using either partial least-squares or factor analysis (Dousseau & Pezolet, 1990; Lee et al., 1990; Sarver et al., 1991). The results obtained by these methods entirely rely on the analysis of valid reference data bases, i.e., the construction of a sufficiently effective calibration matrix of aqueous FT-IR spectra of proteins with known secondary structures. Fallacious interpretations, however, are possible if specific proteins with structures not referenced by the data base are to be analyzed. Apart from this drawback, specific assignments and quantitations are not possible (i.e., the discrimination between different β- or α-helical structures), and, due to the lack of sufficient numbers of X-ray structures of membrane-bound proteins, the reference data base may provide inaccurate results on unknown membrane proteins.

The FT-IR data published by Fong and McNamee (1987) on the basis of two conformation-sensitive IR bands in the so-called skeletal region of the IR spectrum resulted in an exceptionally low helical content (approximately 20–25%), slightly depending on temperature and composition of lipids of the bilayer matrix. However, the poor assignment and specificity of the bands used and the weakly established correlation of these vibrational modes to specific secondary structures might be the reason for uncertainties.

Temperature- and Time-Dependent Changes of the Structure of Acetylcholine Receptor Membranes. Membranes and

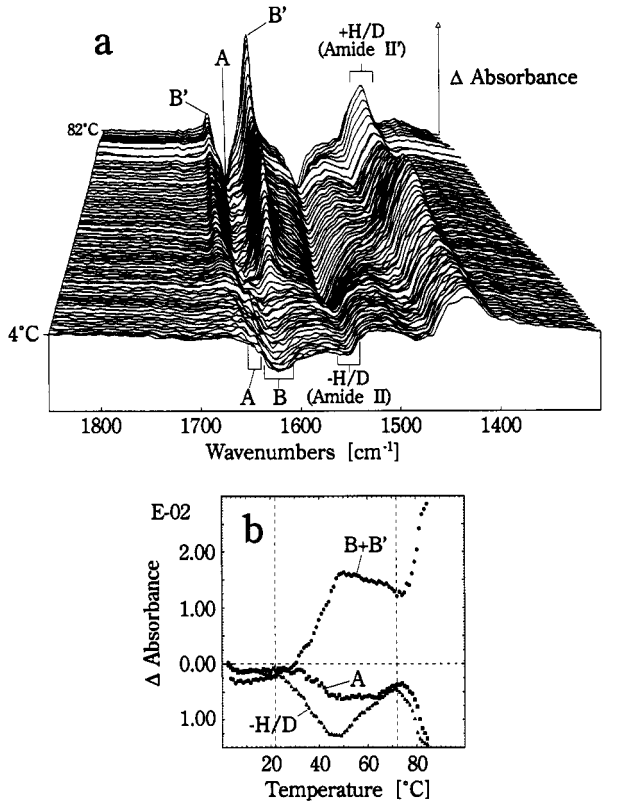

FIGURE 4: Temperature dependence of the secondary structure of the AChR complex in D_2O as observed in the amide I/I' and amide II/II' regions between 1300 and 1800 cm^{-1} by difference spectroscopic techniques. (a) Three-dimensional plot of 4 °C absorbance difference spectra calculated every 1 °C temperature increase. (b) β-Band (1620–1640 cm^{-1}) change as a function of temperature (B+B'); α-helical band (1657 cm^{-1}) change as a function of temperature (A); completion of H–D exchange as a function of temperature (–H/D). Thermal treatment was done by applying a linear temperature gradient of 1 °C temperature increase per 5-min time interval. A, B, B', and H/D stand for α-helices, β-structures, β-aggregation, and hydrogen/deuterium exchange, respectively. Note that change of absorbance ΔA as a function of temperature is plotted in panels a and b, respectively.

proteins undergo temperature-induced phase changes. As far as proteins are concerned, unfolding or denaturation involves major rearrangements of the tertiary structure and distinct changes in the secondary structure. Upon increasing the temperature of the membrane/protein dispersions, the following changes were observed (see Figure 4): (i) The various β-bands were affected first; the α-helical structures represented by the band near 1657 cm^{-1} seemed to be significantly more stable than the β-band. (ii) At temperatures above 20 °C, two new bands appeared near 1620 and 1690 cm^{-1}, respectively. These two bands are specific marker bands for the irreversible, temperature-induced β-aggregation (inter- and/or intramolecularly) of the protein complex (Arrondo et al., 1987; He et al., 1991). (iii) With increasing temperature, completion of H/D exchange started at temperatures above 20 °C, as evidenced by the loss of IR intensity near 1550 cm^{-1}.

The temperature measurements suggested a two-step denaturation process of the AChR complex. Below 20 °C, a small but constant decrease in β-band absorption was detectable, and changes of α-helical structures could not be observed. Possibly, progressing H/D exchange of amide N–H functional groups (see small negative bands near 1550 cm^{-1} and small positive bands near 1440 cm^{-1} in Figure 4a) slightly decreases molar absorptivity of amide I component bands. In consequence, small negative β-bands are observed near 1630–1640 cm^{-1}. Between 20 and approximately 70 °C, a significant change in intensity of the β- and α-bands was observed, and H/D-exchange proceeded. The maximum rate of change of all three parameters took place near 50 °C. The intensity loss of the amide II band near frequency values of 1548 cm^{-1} strongly suggested that the deuteration of shielded protons of α-helical structures occurred. At the same time, minor negative peak intensity near 1651 cm^{-1} (rather than at 1657 cm^{-1}) was observed, indicating that different helical band components might be hidden under the main α-helical band near 1657 cm^{-1}. These components are less resistent to temperature increase and may be located within the globular domain of the complex. The positive peak areas of the "β-aggregation bands" (B' band, see Figure 4) near 1620 and 1690 cm^{-1} are much more intensive than the negative band area near 1651–1657 cm^{-1}. This may be due to differences in molar absorptivities of the two structures (Jackson et al., 1989). In a second step, the complete secondary structure of the protein complex is destroyed. This process is shown by the disappearance of all IR bands attributed to α, β, and turn structures present. The rate of intensity change observed above 70 °C is considerably higher than that observed between 20 and 70 °C. The negative band localized near 1657 cm^{-1} clearly indicates that the membrane-spanning helices are unfolded at these temperatures.

Up to approximately 50 °C, the curves shown in Figure 4b exhibit a relationship similar to that elaborated by ion-gating activity measurements as a function of temperature (Soler et al., 1984) and to that obtained from recent FT-IR/temperature measurements on purified and reconstituted AChR membranes (Fong & McNamee, 1987). Above 50 °C, however, the temperature dependence of the helical and β-sheet marker bands used by Fong and McNamee (1987) suggest only a monotonic decrease in α-helix and β-sheet.

It is also noteworthy that the β-aggregation processes observed by FT-IR are compatible with results obtained by "thermal gel analysis" used to characterize temperature-induced subunit aggregation of the AChR (Soler et al., 1984). Possibly, the first and second protein denaturation steps observed by FT-IR (see curve B+B', Figure 4b) can be related to the different temperatures and kinetics of aggregation of the 60K and 65K subunits, and the 40K and 50K subunits, respectively, as described by Soler et al. (1984).

In order to confirm the experimental results obtained when increasing the temperature continuously, temperature jump measurements between 10 and 25 °C and isothermic, time-dependent changes were investigated by FT-IR difference spectroscopic measurements as well. Figure 5 shows the difference spectra of the receptor vesicles dispersed in H_2O as obtained at constant time intervals 30 and 60 min after a temperature jump from 10 to 25 °C. Both spectra clearly indicate negative bands near 1654 and 1548 cm^{-1} and positive bands near 1620 and 1690 cm^{-1}, respectively. The latter bands, again, show progression of β-aggregation at the expense of the helical structures observed near 1654 cm^{-1}. Additionally, Figure 5 suggests that the negative α-helical band centered around 1654 cm^{-1} is composed of more than a single pure α-helical component.

The temperature-induced frequency shift of symmetric $>CH_2$-stretching helical component band of the phospholipids' acyl chains (data not shown) is a continuous process exhibiting no sign of cooperative acyl chain melting, i.e., a gel to liquid-crystalline phase transition. The frequency values of this particular band range from 2852 to 2854 cm^{-1}, which is indicative of the liquid-crystalline state of biological mem-

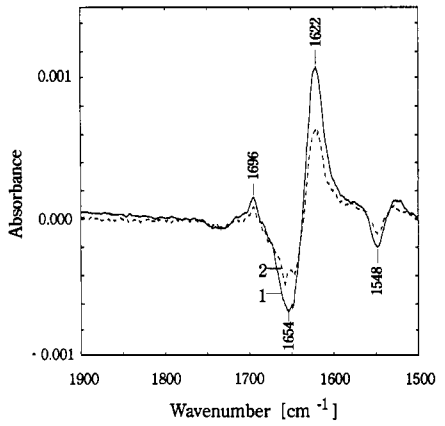

FIGURE 5: Difference spectra as obtained time-dependently from AChR-rich membrane vesicles (in H_2O) after a temperature jump from 10 to 25 °C. (1) Difference spectrum taken 30 min after the temperature jump. (2) Difference spectrum taken 60 min after the temperature jump. Time interval for spectral data acquisition was 30 min each time. Positive peaks indicate increase and negative peaks indicate decrease of structural changes as function of time.

branes. Since the membrane matrix is composed of various phospholipids and large amounts of cholesterol (Fong & McNamee, 1987), the "state of order" of the matrix should be rather low. The occurence of at least three components near 1742, 1726, and 1710–1720 cm^{-1}, respectively, may be related to differences in the strength of hydrogen bonding of ester >C=O groups rather than to the conformational inequivalence of the >C=O functional groups (Casal & Mantsch, 1984; Blume et al., 1988) of the various phospholipids present in AChR-rich membranes (Bhushan & McNamee, 1990). The extremely low frequency component near 1710–1720 cm^{-1} probably arises from strong interactions between cholesterol and some distinct phospholipid >C=O ester groups (Wong et al., 1989; Bhushan & McNamee, 1990).

Conclusions. The technique used here for a semiquantitative analysis of the different secondary structures suggests the predominance of β over α-helical conformations. This is contradictory to the data published by other authors (Fong & McNamee, 1987; Wu et al., 1990). Our technique may overestimate the amount of β-structures at the expense of structures which are generally termed "unordered" or "undefined". However, if we shift, e.g., 5% of the "β-structures" to "unordered" or "undefined" (which is within the maximum error of this technique), the predominance of β-structures would be still preserved. The amount of α-helical structures can only be increased in percentage numbers if one accepts that the 1646–1648-cm^{-1} band component is partly due to specific helical structures, presumably localized within the globular part of the protein protruding into the surrounding water.

Some discrepancy may be explained by the fact that we assigned all IR-band components detectable between 1620 and 1640 cm^{-1} in D_2O/membrane dispersions to β-structures. Components bands, however, near 1640 cm^{-1} might be related to fully hydrated, only weakly chain-interacting, extended conformations (e.g., "open turns", "wide loops"). Such conformations, however, are usually classified as "aperiodic" or "undefined".

The obvious advantage of the FT-IR technique used in this study over other structure-sensitive methods is that it provides additional information on various conformational substructures and allows one to follow changes in protein structure as a function of specific variables. The presence of specific amide I band components suggests that there are different hydrogen-bonded β-structures and helical conformations in the receptor complex.

The samples used for FT-IR analysis are receptor-enriched preparations which still contain the so-called 43K-protein noncovalently bound to the receptor complex (Neubig et al., 1979). Nothing is known about the secondary structure of this particular protein. The amino acid sequence has been recently established (Carr et al., 1987); secondary structure predictions from sequences, however, are not yet available. If one accepts that the 43K-protein is present in stoichiometric amounts, then approximately 10–15% (w/w) of the samples investigated are due to the 43K-protein and should markedly contribute to the spectra observed. If α, β, turn, and random structures of this protein are equal in percentages, only minor uncertainties (3–5%) arise for the quantitative determination of each of the secondary structure classes of the receptor complex. Significant deviations (on the order of 10%), however, can be expected if the 43K-protein is a predominantly α- or β-type protein.

The sensitivity and specificity of the FT-IR technique is best examplified by the temperature- and time-dependent measurement of difference spectra. Our data strongly suggest that the temperature-dependent denaturation of the receptor protein is a two-step process. The temperature range between 20 and 30 °C, where loss of activity of the receptor already starts, is the temperature range where only small structural changes in secondary structure are observed by FT-IR difference spectroscopy accompanied by progressing inter- or intraprotein aggregation phenomena. Large, overall changes of the secondary structure are observed above 50 °C at temperatures where receptor activity is already completely lost.

The results obtained by FT-IR difference spectroscopy suggest that losses of α-helical structures are accompanied by thermally induced protein subunit aggregation. Whether the latter process is causal for the former one cannot be answered by the FT-IR experiments alone. It is, however, reasonable to presume that local conformational changes inducing disruption or distortion of distinct α-helical structures might be the primary event leading to the loss of ion-flux activity. Since the difference spectra shown in Figure 5 indicate changes of more than a single sharp α-helical band, a complex of two or more conformational changes may underlie temperature-induced loss of ion-gate activity.

ACKNOWLEDGMENT

Excellent technical assistance by Mr. Giampiero Bandini and Andrea Stäuble is gratefully acknowledged.

REFERENCES

Arrondo, J. L. R., Mantsch, H. H., Mullner, N., Pikula, S., & Martonosi, A. (1987) *J. Biol. Chem. 262*, 9037–9043.

Aslanian, D., Heidmann, Th., Negrerie, M., & Changeux, J.-P. (1983) *FEBS Lett. 164*, 393–400.

Baenziger, J. E., Miller, K. W., & Rothschild, K. J. (1992) *Biophys. J. 61*, 983–992.

Bandekar, J., & Krimm, S. (1979) *Proc. Natl. Acad. Sci. U.S.A. 76*, 774–777.

Bandekar, J., & Krimm, S. (1980) *Biopolymers 19*, 31–36.

Bhushan, A., & McNamee, M. G. (1990) *Biochim. Biophys. Acta 1027* 93–101.

Blume, A., Hübner, W., & Messner, G. (1988) *Biochemistry 27*, 8239–8249.

Byler, D. M., & Susi, H. (1986) *Biopolymers 25*, 469–487.

Carr, C., McCourt, D., & Cohen, J. B. (1987) *Biochemistry 26*, 7090–7102.

Casal, H. L., & Mantsch, H. H. (1984) *Biochim. Biophys. Acta 779*, 381–401.
Chirgadze, Y. N., & Nevskaya, N. A. (1976a) *Biopolymers 15*, 607–625.
Chirgadze, Y. N., & Nevskaya, N. A. (1976b) *Biopolymers 15*, 627–636.
Claudio, T. (1989) in *Frontiers in Molecular Biology: Molecular Neurobiology Volume*, pp 63–142, IRL Press, Oxford.
Claudio, T., Ballivet, M., Patrick, J., & Heinemann, S. (1983) *Proc. Natl. Acad. Sci. U.S.A. 80*, 1111–1115.
DiPaola, M., Dyajkowski, C., & Karlin, A. (1989) *J. Biol. Chem. 264*, 15457–15463.
Dong, A., Huang, P., & Caughey, W. S. (1990) *Biochemistry 29*, 3303–3308.
Dousseau, F., & Pezolet, M. (1990) *Biochemistry 29*, 8771–8779.
Downer, N. W., Bruchman, T. J., & Hazzard, J. H. (1986) *J. Biol. Chem. 261*, 3640–3647.
Finer-Moore, J., & Stroud, R. M. (1984) *Proc. Natl. Acad. Sci. U.S.A. 81*, 155–159.
Fong, T. M., & McNamee, M. G. (1987) *Biochemistry 26*, 3871–3880.
Görne-Tschelnokow, U., Hucho, F., Naumann, D., Barth, A., & Mäntele, W. (1992) *FEBS Lett. 309*, 213–217.
Guy, H. R., & Hucho, F. (1987) *Trends Neurosci. 10*, 318–321.
Haris, P. I., Coke, M., & Chapman, D. (1989) *Biochim. Biophys. Acta 995*, 160–167.
He, W.-Z., Newell, W. R., Haris, P. I., Chapman, D., & Barber, J. (1991) *Biochemistry 30*, 4552–4559.
Hucho, F., & Hilgenfeld, R. (1989) *FEBS Lett. 257*, 17–23.
Jackson, M., Haris, P. I., & Chapman, D. (1989) *Biochim. Biophys. Acta 998*, 75–79.
Karlin, A. (1991) *The Harvey Lectures, Series 85*, 71–107.
Kauppinen, J. K., Moffat, D. J., Mantsch, H. H., & Cameron, D. G. (1981) *Appl. Spectrosc. 35*, 271–276.
Kennedy, D. F., Crisma, M., Toniolo, C., & Chapman, D. (1991) *Biochemistry 30*, 6541–6548.
Krikorian, J. G., & Bloch, R. J. (1992) *J. Biol. Chem. 267*, 9118–9128.
Krimm, S. (1962) *J. Mol. Biol. 4*, 528–540.
Kunath, W., Giersig, M., & Hucho, F. (1989) *Electron Microsc. Rev. 2*, 349–366.
Kyte, J., & Doolittle, R. F. (1982) *J. Mol. Biol. 157*, 105–132.
Lee, D. C., Haris, P. I., Chapman, D., & Mitchell, R. C. (1990) *Biochemistry 29*, 9185–9193.
Mantsch, H. H., Surewicz, W. K., Muga, A., Moffatt, D. J., & Casal, H. L. (1989) *Proc. SPIE-Int. Soc. Opt. Eng. 1145*, 580–581.
Marquardt, D. W. (1963) *J. Soc. Ind. Appl. Math. 11*, 431–441.
McCarthy, M. P., & Stroud, R. M. (1989) *Biochemistry 28*, 40–48.
Mielke, D. L., & Wallace, B. A. (1988) *J. Biol. Chem. 263*, 3177–3182.
Moore, W. M., Holladay, L. A., Puett, D., & Brady, R. N. (1974) *FEBS Lett. 45*, 145–149.
Naumann, D., Schultz, C., Sabisch, A., Kastowsky, M., & Labischinski, H. (1989) *J. Mol. Struct. 214*, 213–246.
Neubig, R. R., Krodel, E. K., Boyd, N. D., & Cohen, J. B. (1979) *Proc. Natl. Acad. Sci. U.S.A. 76*, 690–694.
Nevskaya, N. A., & Chirgadze, Y. N. (1976) *Biopolymers 15*, 637–648.
Rial, E., Muga, A., Valpuesta, J. M., Arrondo, J. L. R., & Goni, F. M. (1990) *Eur. J. Biochem. 188*, 83–89.
Sarver, R. W., Jr., & Krueger, W. C. (1991) *Anal. Biochem. 194*, 89–100.
Schiebler, W., & Hucho, F. (1978) *Eur. J. Biochem. 85*, 55–63.
Soler, G., Mattingly, J. R., Jr., & Martinez-Carrion, M. (1984) *Biochemistry 23*, 4630–4636.
Stroud, R. M., McCarthy, M. P., & Shuster, M. (1990) *Biochemistry 29*, 11009–11023.
Surewicz, W. K., & Mantsch, H. H. (1988) *Biochim. Biophys. Acta 952*, 115–130.
Wong, P. T. T., Capes, S. E., & Mantsch, H. H. (1989) *Biochim. Biophys. Acta 980*, 37–41.
Wu, C.-S. C., Sun, X. H., & Yang, Y. T. (1990) *J. Protein Chem. 9*, 119–126.
Yager, P., Chang, E. L., Williams, R. W., & Dalziel, A. W. (1984) *Biophys. J. 45*, 26–28.